



## Automated detection methods for architectural distortions around skinline and within mammary gland on mammograms

T. Matsubara<sup>a,\*</sup>, T. Ichikawa<sup>b</sup>, T. Hara<sup>b</sup>, H. Fujita<sup>b</sup>, S. Kasai<sup>c</sup>,  
T. Endo<sup>d</sup>, T. Iwase<sup>e</sup>

<sup>a</sup> Nagoya Bunri University, 365 Maeda, Inazawa-cho, Inazawa 492-8520, Japan

<sup>b</sup> Gifu University, 1-1 Yanagido, Gifu 501-1193, Japan

<sup>c</sup> Konica Corporation, 1 Sakura-machi, Hino 191-8511, Japan

<sup>d</sup> National Hospital of Nagoya, 4-1-1 Sannomaru, Naka-ku, Nagoya 460-0001, Japan

<sup>e</sup> Cancer Institute Hospital, 1-37-1 Kamiikebukuro, Toshima, Tokyo 170-8455, Japan

Received 13 March 2003; received in revised form 13 March 2003; accepted 17 March 2003

---

### Abstract

The architectural distortion is a very important finding in interpreting breast cancers as well as microcalcification and mass on mammograms. However, it is more difficult for physicians to detect architectural distortion than microcalcification and mass. The purpose of this study is to develop two detection approaches for architectural distortions existing around skinline and within mammary glandular tissues. The detection methods for depressed areas around skinline consisted of three steps. The binarization technique was performed to extract the mammary gland region. In order to determine suspect areas, the top-hat processing was performed. The false positives were eliminated by the features of their sizes and positions. The distorted areas within mammary gland region were detected by the following steps. The structure of mammary gland was extracted by using curvature. The candidates were determined by concentration index. The false positives were eliminated by their isotropy indexes, sizes, pixel values and contrast. Our image database consisted of 17 cases with focal retraction areas around skinlines (case A) and 38 cases with architectural distortions within mammary glands (case B). As a result, the sensitivities were 94% and 84% in case A and case B, respectively. It was concluded that our methods were effective to detect architectural distortions.

© 2003 Elsevier Science B.V. and CARS. All rights reserved.

*Keywords:* Architectural distortion; Mammogram; Computer-aided diagnosis; Automated detection; Image analysis

---

\* Corresponding author. Tel.: +81-587-23-2400; fax: +81-587-21-2844.

E-mail address: tomoko@nagoya-bunri.ac.jp (T. Matsubara).

## 1. Introduction

We have been developing a synthetic CAD system to automatically detect and classify benign and malignant of both microcalcifications and masses, to extract both skinline and pectoral muscle, and to assess the density of fibroglandular breast tissue on digitized mammograms. We also have confirmed the validity of the detection performance of our CAD system by the validation test with over 10,000 images because the performance of the system showed high sensitivity and specificity in consistency test by using a limited number of cases. It was found that some microcalcifications and masses missed by radiologists were detected by our CAD system. However, the detection method of architectural distorted area of mammary regions was not implemented in our CAD scheme at this time.

The architectural distortion is a very important finding in interpreting breast cancers as well as microcalcification and mass on mammograms. In addition, it sometimes appears at the previous stage of obvious mass shadow. Because it is difficult to detect spiculated mass in dense breast on mammogram, it is necessary to detect spicula as architectural distortion. However, it is more difficult for physicians to detect architectural distortion than microcalcification and mass [1].

The architectural distortions can be classified into two types: the one existing around skinline and the other within mammary glandular tissues. Fig. 1 shows the typical patterns of distorted areas with sketches by a physician.

The purpose of this study is to develop two methods for detecting architectural distortions.

## 2. Material and methods

The automated scheme developed for the detection of architectural distortion consisted of two steps: (i) determination of architectural distortion candidates around skinline and

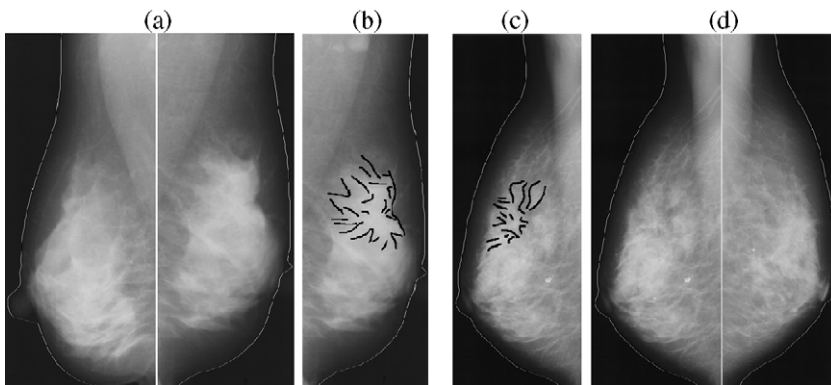


Fig. 1. Examples of architectural distortions. Two typical types distortions existing around skinline (a) and within mammary glandular tissues (d). (b) and (c) are sketches of distortion areas in (a) and (d), respectively.

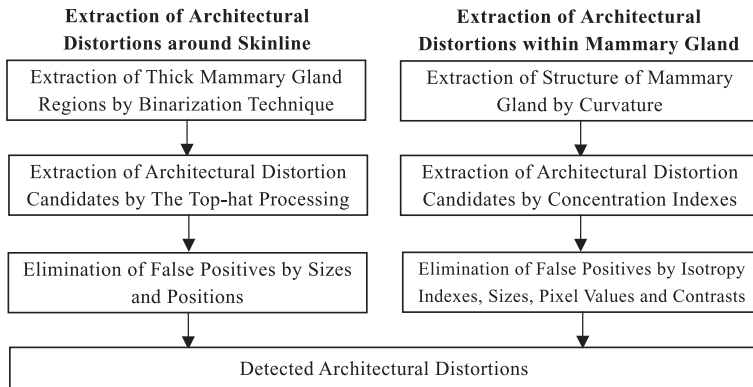


Fig. 2. Extraction flowchart for architectural distortions.

elimination of false positives [2] and (ii) determination of architectural distortion candidates within mammary glandular tissue and elimination of false positives. Extraction flowchart for architectural distortions is shown Fig. 2. Each step in our scheme is explained in order as follows.

2.1. Determination of architectural distortion candidates around skinline and elimination of false positives

The contours of normal glandular tissue around skinline tend to be smooth lines; on the other hand, those of distorted one were depressed. Fig. 3 shows simplified illustrations of normal (a) and abnormal (b, c) images. The detection target at this first process was the depressed area (b) on the outline of mammary gland region around skinline.

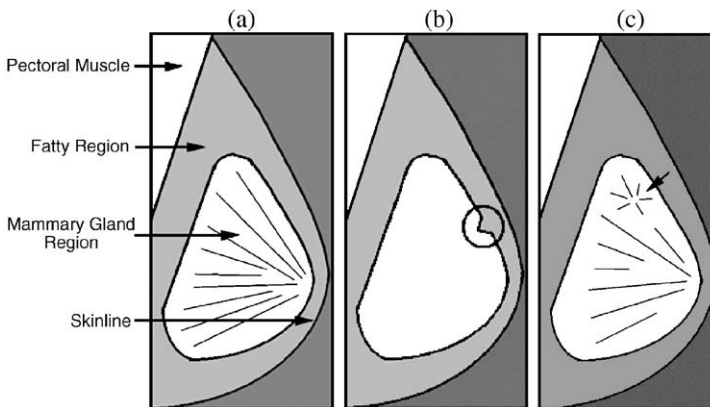


Fig. 3. Simplified illustrations of (a) normal image, (b) abnormal images with architectural distortions (focal retraction) around skinline indicated by a circle, and (c) within mammary gland region indicated by an arrow.

First, the dynamic-range compression technique was carried out within the breast region in order to compensate for the difference of the background density due to the breast thickness [3]. The thick mammary gland regions were extracted by using binarization technique [4]. The threshold at this process was determined by referring to the density of pectoral muscle region to avoid the misconfiguration of the threshold caused by the density difference of radiographed conditions on mammograms. Second, the top-hat processing based on morphological operators was applied to determine the suspect depressed regions around skinline [5]. The procedure of top-hat processing was achieved by subtracting the opening-operated image from the original image. In our experiments, we chose linear structures in seven directions whose angles were  $45^\circ$ ,  $60^\circ$ ,  $75^\circ$ ,  $90^\circ$ ,  $105^\circ$ ,  $120^\circ$  and  $135^\circ$  to fit to the shape of outlines. Finally, the feature analyses were performed in order to reduce the false-positives. The candidates whose sizes were larger than  $S_{\max}$  or smaller than  $S_{\min}$  or not existing around skinline were eliminated. This process for architectural distortions existing around skinline is illustrated in Fig. 4.

## 2.2. Determination of architectural distortion candidates within mammary glandular tissue and elimination of false positives

The distributions of mammary gland were approximated to linear structures. Those within normal breast were toward the nipple; on the other hand, those within abnormal breast were toward the suspect area. Fig. 3(c) shows a simplified illustration of architectural distortion within mammary gland region.

First, the linear structures of mammary gland were extracted by the mean curvature whose sign showed the downward or upward curved surface at a point. The mean curvature of mammary gland showed the positive. Second, the suspect area was

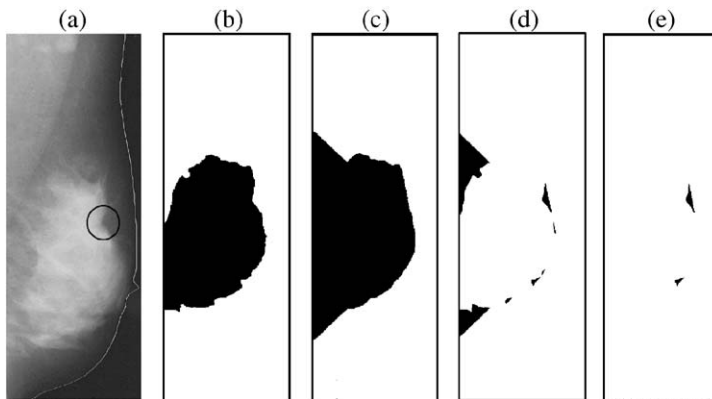


Fig. 4. Extraction flow diagram for architectural distortion existing around skinline. (a) An original image with distorted area indicated by circle. (b) Extracted mammary gland region in (a). This region contains focal retraction area. (c) The smoothed image obtained by the closing of (b) by structuring elements. (d) The difference image contains the candidates of distorted areas. (e) Elimination of false positives by the features of their sizes and positions. The upper and lower candidates are true positive and false positive, respectively.

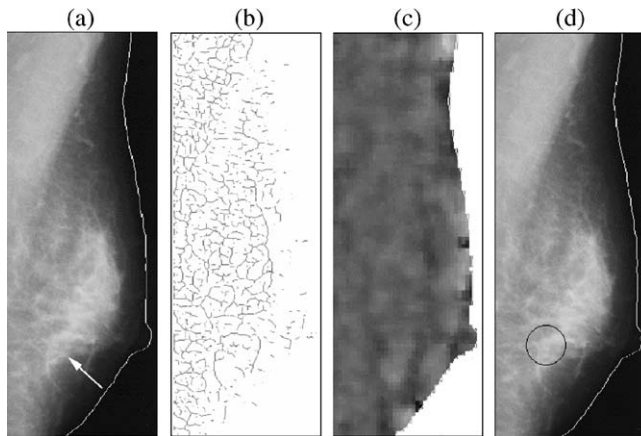


Fig. 5. Extraction flow diagram for architectural distortion within mammary gland region. (a) An original image with architectural distortion indicated by an arrow. (b) The extracted structure of mammary gland by using curvature. (c) The image of concentration index of (b). Black area is high concentration index. (d) Detected area indicated by a circle.

determined by concentration index calculated by lengths, directions, and distances of the linear structures. The concentration index of distorted area has a high value because the linear structures of mammary gland were toward the suspect area. Finally, the feature analyses were performed in order to reduce the false positives. The concentration indexes not only of distorted areas but also of line structures such as blood vessels have high values. The false positives such as blood vessels were eliminated by the isotropy index that could classify line structures of several directions and those of one direction. The candidates whose sizes were small were eliminated. By comparing the distorted regions with normal ones, the distorted mammary gland tissue tended to be light areas (white regions on films); on the other hand, the surrounding regions around the architectural distortions were dark because these areas contained much fat tissue. The false-positive candidates were eliminated by density analysis. This extraction process for architectural distortions within mammary gland region is demonstrated in Fig. 5.

The residual candidate was finally indicated by a circle as “true” architectural distortion.

### 3. Results

Our image database consisted of 17 cases with focal retraction areas around skinlines (case A) and 38 cases with architectural distortions within mammary glands (case B). To our knowledge, it was the maximum database of architectural distortions in the world. An experienced radiologist verified the diagnostic sketches and commented in detail on all cases used in our studies. As a result, the sensitivities were 94% and 84% with 2.3 and 2.4 false-positives per image in case A and case B, respectively.

#### **4. Summary**

We developed the automated detection methods of architectural distortions on mammograms based on the top-hat processing and the concentration index of mammary gland. It was concluded that our methods were effective because the architectural distortions were detected correctly with few false positives per image. However, it was not possible to detect the pale architectural distortions by either method.

For the future work, it is necessary to add new algorithms to detect the pale distorted areas and to decrease false positives.

#### **Acknowledgements**

This work was supported in part by the Ministry of Health, Labour and Welfare under a Grant-In-Aid for Cancer Research, and in part by the Ministry of Education, Culture, Sports, Science and Technology under a Grant-In-Aid for Scientific Research, Japanese Government.

#### **References**

- [1] Y. Hatanaka, T. Matsubara, H. Hara, N. Shinohara, D. Fukuoka, H. Fujita, T. Endo, A comparison between physicians' interpretation and a CAD system's cancer detection by using a mammogram database in a physicians' self-learning course, *Jpn. J. Radiol. Technol.* 58 (3) (2000) 375–382.
- [2] T. Matsubara, D. Yamazaki, T. Hara, H. Fujita, S. Kasai, T. Endo, T. Iwase, Development of automated detection methods for architectural distortions on mammograms, *Proceedings of the 16 the International Congress and Exhibition on Computer Assisted Radiology and Surgery (CARS2002)* (2002) 1102.
- [3] T. Hara, Y. Lee, H. Fujita, Breast peripheral-area enhancement processing for mammogram CAD by using dynamic-range compression, *Med. Imaging Inf. Sci.* 13 (2) (1996) 78–82.
- [4] T. Matsubara, D. Yamazaki, H. Fujita, T. Hara, T. Iwase, T. Endo, An automated classification method for mammograms based on evaluation of fibroglandular breast tissue density, *Proceedings of IWDM 2000—5th International Workshop on Digital Mammography* (2000) 737–741.
- [5] H. Kobatake, *Morphology*, Corona Publishing, Tokyo, 1996.